



Cite this: *Mater. Adv.*, 2021, 2, 448

Chemisorption of CO₂ on diaminated silica as bicarbonates and different types of carbamate ammonium ion pairs

Anthony E. Szego, Aleksander Jaworski and Niklas Hedin  *

The chemisorption of CO₂ on aminated silica has a rich chemistry, and its details are important to research in relation to CO₂ capture and catalytic chemistry. In this study, such chemisorption was investigated on aminated and diaminated silica with ¹H and ¹³C solid state nuclear magnetic resonance (NMR) spectroscopy under dry and wet conditions. Fast magic-angle spinning (MAS) allowed us to obtain high resolution spectra. Porous silica was modified into a monoaminated version using (3-aminopropyl)triethoxysilane (APTS) and a diaminated one by using 3-(2-aminoethylamino)propyltriethoxysilane (AEAPTS). From the corresponding NMR spectra we could conclude that, under dry conditions, CO₂ chemisorbed as carbamic acid and carbamate ammonium ion pairs and gave similar spectra for both directly-excited ¹³C and under cross-polarization (CP) ¹H¹³C MAS NMR. Under wet conditions, direct excitation and ¹H¹³C CPMAS NMR showed that carbamate ammonium ion pairs formed along with bicarbonates (HCO₃⁻). For the wet conditions, the ¹³C and ¹H NMR spectra were especially well resolved, and we could detect two different types of carbamate ammonium ion pairs forming on the diaminated silica. We conclude that carbamate ammonium ion pairs and HCO₃⁻ moieties can be detected by ¹H¹³C MAS NMR, at least qualitatively, in addition to the more time consuming direct excitation.

Received 31st August 2020,
Accepted 5th December 2020

DOI: 10.1039/d0ma00658k

rsc.li/materials-advances

1. Introduction

Pilot plants for the capturing of carbon dioxide (CO₂) are based on the use of established scrubbing technology with aminated solvents that allows the capturing and relatively easy release/regeneration of the captured CO₂.^{1,2} There is a major issue with these practices though, which include the high energy demand for regeneration of the solvent, corrosion of equipment, and the evaporation and leaching of the amine or associated degeneration products. Immobilized amines on porous solid supports could possibly reduce the energy required for regeneration, limit the corrosion, and the evaporation of the amines.³⁻⁶

Mesoporous silica, in particular, has been very popular as a solid to immobilize amine functions and reduce corrosion and leaching.⁷⁻¹⁰ One of three ways can be used to modify silica with amines: by physical immobilization of compounds on the surface, chemical tethering, or crosslinking of polyamines throughout the pores of the silica. The amine-modified solid adsorbents – similarly to liquid amines – have been shown to exhibit a highly selective uptake of CO₂ and a high capacity for CO₂ uptake at low partial pressures of the CO₂.¹¹⁻¹³

Despite the advantages these types of amine-modified sorbents have, full mechanistic understanding of the reaction of the amines with CO₂ has yet to be achieved.¹⁴⁻²⁰ It is known from previous works that in the reactions between CO₂ and amines in the presence of water, three main species are involved: carbamic acid, carbamate ammonium ion pairs, and bicarbonates (HCO₃⁻). Even though the formation of HCO₃⁻ has been shown to enhance the so-called amine efficiency,²¹⁻²³ the formation of these species could potentially be considered a drawback in the context of CO₂ capture due to the expected higher energy required for the regeneration of the material, and overall reduced adsorption and desorption rates, despite the increase in sorption capacity.²⁴⁻²⁶

The existence of HCO₃⁻ in CO₂ chemisorption reactions on moist solid amines has been questioned in the past.^{14,15,23,27-29} In light of findings from the liquid state amine–CO₂–H₂O chemistries,³⁰⁻³² it would seem obvious that HCO₃⁻ should form within pores of moist amine-modified sorbents. However, it has not been easy to detect HCO₃⁻ by solid-state NMR and, also, its IR signatures have been difficult to assign.¹¹ Solid-state NMR is used extensively to characterize chemisorption products in general, because it can determine the structures of non-crystalline systems.^{33,34} This versatility also allows the method to be used in the identification and quantification of the analyzed products, *in situ* and *ex situ*.^{14,33,35} In NMR, in



particular, the ^{13}C chemical shift of HCO_3^- appears at a range of values, depending on the environment that contributes to the shielding experienced by the ^{13}C nucleus.³⁶ As a result, its NMR resonance may be masked by that of potentially more prominent carbamate or carbamic acid resonances. For this reason, the samples presented in this paper have been divided into “wet” and “dry” samples, as the absence of H_2O is known to restrict the formation of HCO_3^- .³⁷ Carbonates (CO_3^{2-}) will not be observed in the present paper because conditions that favor its formation ($\text{pH} > 10.3$) are not present.

Despite the aforementioned debate regarding the involvement of HCO_3^- in these types of systems, previous work done recently by Chen *et al.*²⁷ was able to find and assign a peak to this species. They could unambiguously show with the so called direct polarization ^{13}C NMR method that HCO_3^- formed when the samples had been subjected to liquid H_2O . The fast dynamics and, in our interpretation, the liquid-like character of the formed HCO_3^- dissolved in the pores largely filled with H_2O , were the reasons why HCO_3^- was not easily detected at room temperature in that study and gave convincing insight as to why it had not earlier been detected by the more commonly used cross-polarization method, here called as $\{^1\text{H}\}^{13}\text{C}$ NMR. The absence of the $\{^1\text{H}\}^{13}\text{C}$ NMR signal for HCO_3^- in most studies has likely been related to that the details of the cross-polarization dynamics associated to its presumed liquid-state-type character are not fully taken into account, which in turn will hinder an effective magnetization transfer. H_2O adsorbs in significant amounts on amine-modified adsorbents.^{15,22}

The work presented here is meant to further contribute to this exploration of the presence of HCO_3^- in these systems. We show that $\{^1\text{H}\}^{13}\text{C}$ NMR could be used at least qualitatively to identify HCO_3^- for samples being rich in co-adsorbed H_2O and that two different types of carbamates formed in moist diaminated silica on the chemisorption of CO_2 .

2. Materials and synthesis

Chromatographic particles of porous silica, Davisil LC60 (Grace Davison), was used as a porous support. It had a particle size of 40–63 μm , and a surface area of $550 \text{ m}^2 \text{ g}^{-1}$. The support was used as received after a drying treatment at a temperature of 110 °C for 16 h. Analytical-grade toluene ([CAS: 108-88-3], Sigma-Aldrich 99.8%) with 0.03 wt% H_2O was used. The porous silica was modified with (3-aminopropyl)triethoxysilane (APTS) ([CAS: 919-30-2], Sigma-Aldrich >98%) and 3-(2-aminoethylamino)propyltriethoxysilane (AEAPTS) ([CAS: 5089-72-5], Sigma-Aldrich >96%). Labelled $^{13}\text{CO}_2$ ([CAS: 1111-72-4], Sigma-Aldrich 99 atm% ^{13}C) was used for the NMR experiments.

2.1. Modifications with propylamine and a diamine groups

The porous silica was dried at a temperature of 110 °C before synthesis, and the synthesis procedure was adapted from methods previously reported in the group.³⁸ In summary, for each synthesis 3 grams of porous silica and 180 cm^3 of toluene were added to a three-necked flask equipped with a Dean–Stark

reflux condenser. The solutions were heated to 50 °C under stirring for 30 min; a previously established amount of H_2O was added and the mixtures were refluxed for a period of 1 h. After this period had elapsed, the required amount of silane monomer was added (APTS or AEAPTS) and left to reflux for 24 h. Finally, the solid was filtered off, washed with ethanol (50 $\text{cm}^3 \times 3$) and toluene (50 $\text{cm}^3 \times 2$) and dried overnight at a temperature of 100 °C. The sample modified with the monoamine monomer is called Silica_APTS, and the one with the diamine monomer Silica_AEAPTS.

3. Characterization

3.1. Solid state nuclear magnetic resonance

In order to ensure that all chemisorbed species formed were detected, two protocols for the ^{13}C NMR and one protocol for the ^1H NMR were used for each sample. We studied ^1H and ^{13}C NMR responses using direct excitation, and $\{^1\text{H}\}^{13}\text{C}$ NMR using cross-polarization (CP). 99% ^{13}C -enriched CO_2 was used for the experimentation. All NMR experiments were performed at the magnetic field strength of 14.1 T (Larmor frequencies of 600.1 and 150.9 MHz for ^1H and ^{13}C , respectively) with a Bruker Avance-III spectrometer.

^1H MAS NMR experiments were carried out with a 1.3 mm probehead at the MAS rate of 60.00 kHz. Acquisitions involved rotor-synchronized, double-adiabatic spin-echo sequence with a 90° excitation pulse of 1.1 μs , followed by two 50.0 μs tan h per tan high-power adiabatic pulses with 5 MHz frequency sweep.^{39,40} 256 signal transients with 5 s relaxation delay were collected for each sample. Rotors were filled with powdered Silica_APTS and Silica_AEAPTS and pre-treated under high dynamic vacuum (turbo pump) on the degas port of a Micrometrics ASAP2020 volumetric adsorption analyzer at a temperature of 110 °C. After this degassing, the Silica_APTS and Silica_AEAPTS were divided into “dry” and “wet” samples. The dry samples were subjected to 1 bar of CO_2 enriched in ^{13}C , at 25 °C, for a period of 48 hours, and, finally, the rotors were capped in a glovebox under a continuous flow of N_2 for these dry samples. For the wet samples, the degassed rotors were conditioned in an enclosed environment, for 16 h, where the air was saturated with H_2O after which they were subjected to 1 bar of CO_2 enriched in ^{13}C in a fashion similar to that of the dry samples. The rotors were rapidly capped before each measurement within the glovebox.

Direct excitation ^{13}C and $\{^1\text{H}\}^{13}\text{C}$ CPMAS NMR spectra were recorded with a 4 mm probehead and 14.00 kHz MAS rate. ^{13}C MAS NMR spectra involved a 4.0 μs 90° excitation pulse and Spinal64 ^1H decoupling sequence⁴¹ operated at proton nutation power of 65 kHz. 128 signal transients with 300 s relaxation delay were collected. For $\{^1\text{H}\}^{13}\text{C}$ CPMAS acquisitions Hartmann–Hahn matched radiofrequency fields were applied for a contact interval of 0.5 ms and employed the same proton decoupling scheme. 16384 signal transients with 2 s relaxation delay were collected. Chemical shifts are referenced with respect to neat tetramethylsilane (TMS).



3.2. CO₂ adsorption measurements

Adsorption and desorption isotherms of pure CO₂ on Silica_APTS and Silica_AEAPTS were measured at a temperature of 0 °C using a Micrometrics ASAP2020 volumetric adsorption analyzer. These were compared to a sample of unmodified silica that had undergone the same toluene treatment without the inclusion of silane monomer. The volumetric uptake of CO₂ was measured at CO₂ pressures from 0.001 to 1 bar under equilibrium conditions. Thermal control was achieved by immersing the samples in a Dewar flask filled with ~3 dm³ of H₂O and ice, which equilibrated the temperature to 0 °C. For these measurements, the samples were pretreated under high dynamic vacuum conditions at 110 °C for 10 h before experimentation.

3.3. Thermogravimetric analysis

Thermogravimetric analysis (TGA) was used to record the mass loss on heating Silica_APTS and Silica_AEAPTS using a TA Instruments Discovery (TA Instruments, Stockholm, Sweden) thermobalance in dry air, for which samples were heated from 50 to 950 °C at a rate of 10 °C min⁻¹ in a platinum cup.

4. Results and discussion

4.1. Solid-state NMR

In order to identify the species formed after the chemisorption of CO₂ on Silica_APTS and Silica_AEAPTS under “wet” and “dry” conditions, isotopic labelling in ¹³C was used together with directly-excited ¹³C, {¹H}¹³C, and ¹H MAS NMR spectroscopy. Under dry conditions, carbamate ammonium ion pairs and carbamic acid groups were detected on Silica_APTS and Silica_AEAPTS, and the corresponding directly-excited ¹³C and {¹H}¹³C MAS NMR spectra in Fig. 1 were similar. The broad resonance at a ¹³C chemical shift of about 165 ppm was assigned to the carbamate part of carbamate ammonium ion pairs,^{14,42–44} and the broad resonance at about 160 ppm to what seems to be carbamic acid.^{14,42,44,45} Under wet conditions, carbamate ammonium ion pairs and HCO₃⁻ species were detected in the directly excited ¹³C and {¹H}¹³C NMR spectra in Fig. 1. The narrow ¹³C NMR signals at chemical shifts of 161.4 and 161.7 ppm were assigned to HCO₃⁻ using the assignments of Chen *et al.*²⁷ supported by assignments in related liquid state systems.⁴⁶ The relative signal intensities for HCO₃⁻ in Fig. 1 were much smaller for the {¹H}¹³C NMR spectra as compared to those observed in the directly excited ¹³C NMR spectra for both Silica_APTS and Silica_AEAPTS, which is in line with the general findings of the study by Chen *et al.*²⁷ about a reduced or vanishing cross-polarization efficiency for these HCO₃⁻. We ascribe that we, in contrast to Chen *et al.*, were able to clearly detect the HCO₃⁻, also at room temperature, either to the delicate details in the cross-polarization conditions or that we had equilibrated the samples with gaseous H₂O (at 100% relative humidity). Note that the relative ¹³C NMR signal intensity for the HCO₃⁻ in the directly excited ¹³C NMR spectra

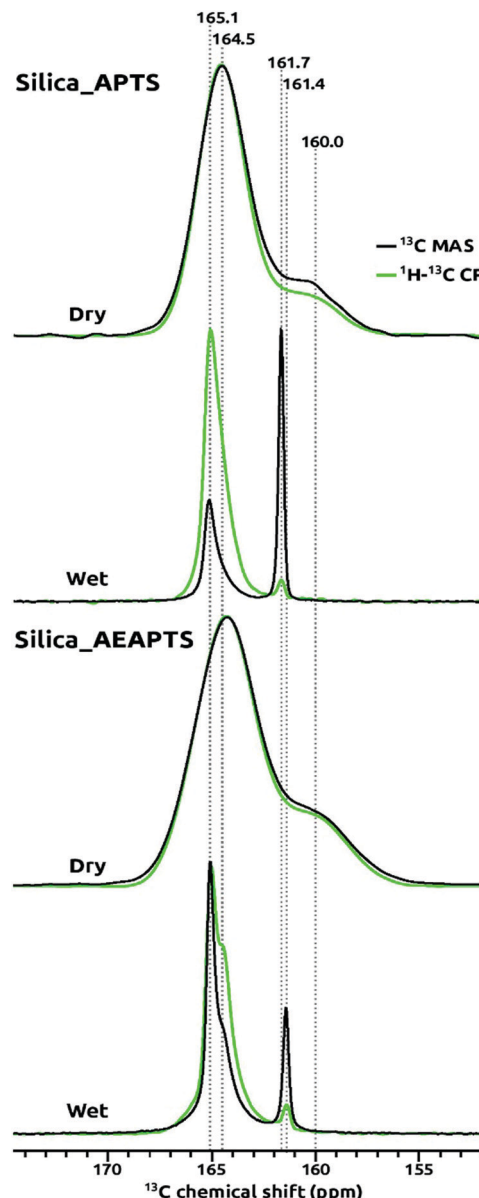


Fig. 1 ¹³C solid-state NMR spectra recorded in wet and dry conditions for samples modified with (3-aminopropyl)triethoxysilane (Silica_APTS) and 3-(2-aminoethylamino)propyltriethoxysilane (Silica_AEAPTS). Black lines correspond to direct excitation ¹³C NMR and the green ones to cross-polarization (¹H)¹³C NMR. Labelled ¹³CO₂ gas was used.

was higher for Silica_AEAPTS than for Silica_APTS, which was related to a higher loading of organics in Silica_AEAPTS.

Interestingly, signals in the ¹³C MAS NMR spectra for the chemisorbed moieties of CO₂ under wet conditions were much narrower than for those recorded under dry conditions, as can be seen by comparing the line widths for the respective ¹³C NMR signals in Fig. 1. Our interpretation of the narrower distributions of ¹³C NMR chemical shifts for the wet samples relates to the fact that the mobility of the chemisorbed CO₂ as both carbamates and HCO₃⁻ was much higher under the wet conditions as compared to dry conditions. The co-adsorbed H₂O appears to solvate the tethered amines and their chemisorbed CO₂.

For the HCO_3^- , we even expect that a large fraction was dissolved in the H_2O adsorbed on the samples. Amine modified silica adsorbs H_2O well already at low relative humidity,^{15,22} and we had subjected Silica_APTs, and Silica_AEAPTS to 100% relative humidity before the chemisorption of $^{13}\text{CO}_2$ for the wet samples. Under the dry conditions the spectroscopic dispersions of the carbamate moieties on Silica_APTs, and Silica_AEAPTS seem to have been larger and hence the corresponding ^{13}C NMR resonances were broader. It is important to mention that the relatively sharp signals, especially for the HCO_3^- species, has been scarcely seen, if ever, for these type of materials.

As mentioned, carbamate ammonium ion pairs formed on chemisorption of CO_2 under both dry and wet conditions for Silica_APTs and Silica_AEAPTS, in addition to carbamic acid and HCO_3^- that formed in parallel under dry and wet conditions, respectively. HCO_3^- moieties are not expected to be observed under dry conditions since H_2O plays a role in the H-transfer that results in their formation, compare with Scheme 1(a).

Notably, in the Silica_AEAPTS wet sample, the ^{13}C NMR signal at ~ 165 ppm ascribed to the carbamate species were split in two, *cf.* Fig. 1. This shoulder is thought to be due to the possibility of different moieties of carbamates being able to form in this case since the sample contains two amine groups, one being primary and the other being secondary¹⁴ (Scheme 1(b)).

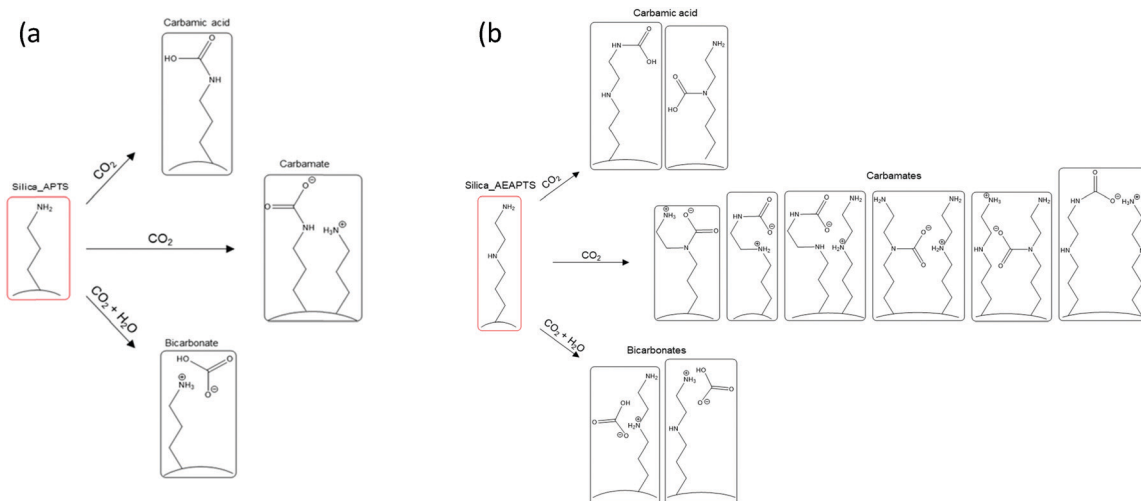
Also in the ^1H NMR spectra, the NMR resonances were narrower for the wet samples than for the dry ones, as can be observed from the ^1H NMR signals in Fig. 2. This narrowing was ascribed to a more liquid-like character for the tethered amines and the chemisorbed CO_2 in the wet samples. Co-adsorbed H_2O has been shown to liberate the motion of the tethered and crosslinked molecules.⁴⁷ It is also known that amine-modified silica materials have a higher hydrophilicity than bare silica leading to a situation where the conditions of the wet samples in this study were very close to those of

liquid-filled pores, resulting in an enhancement of the mobility of the species.⁴⁸

In the ^1H NMR region of 0.6–4 ppm in Fig. 2, signals corresponding to the alkyl chains of the condensed moieties on the porous silica were observed. The ^1H NMR spectra were similar for the Silica_APTs and Silica_AEAPTS samples due to the similar chemical nature of the condensed or tethered amines, and the resolution, albeit high under wet conditions, did not make it possible to distinguish every ^1H NMR signal for each of the different CH_2 groups in the Silica_AEAPTS sample. Nonetheless it was still possible to attribute the ^1H NMR resonances at around 0.6 ppm to the $-\text{CH}_2-$ species directly bonded to silicon atoms. At around 1.5 ppm, the signals for the $\beta\text{-CH}_2-$ groups were observed, and at about 2.6–3.0 ppm the signals for the $\alpha\text{-CH}_2-$ groups, next to the amine groups, were observed. For Silica_AEAPTS, the ^1H NMR signal for the $\alpha\text{-CH}_2-$ was split in the spectrum for the wet sample. It is noted that the diamine (AEAPTS) had three $\alpha\text{-CH}_2-$ group, two of which were connected to the secondary amine and one to the primary amine. Hence, the signal at 3.0 ppm was tentatively assigned to the $\alpha\text{-CH}_2-$ group of the primary amine. At 4.8–5.0 ppm, the ^1H NMR resonance for adsorbed H_2O was observed for the Silica_APTs and Silica_AEAPTS samples, and the signal intensities were particularly intense for the wet samples. The $-\text{NH}-$ and $-\text{NH}_2$ groups were, however, not detected directly in the ^1H NMR spectra for Silica_APTs nor Silica_AEAPTS, likely due to chemical exchange with H_2O or Si-OH groups in both the dry and wet samples.

4.2. CO_2 adsorption measurements

Adsorption isotherms of CO_2 for pure and amine modified silica are shown in Fig. 3, all of them following the treatment with toluene for comparison. At low pressures (0–0.02 atm) of CO_2 , the amine modified sorbents showed a higher uptake of CO_2 than the unmodified silica did, with the diaminated sample (Silica_AEAPTS) showing the highest level of CO_2



Scheme 1 Scheme and structure of possible species formed during CO_2 uptake of (a) the monoaminated Silica_APTs and (b) the diaminated Silica_AEAPTS.

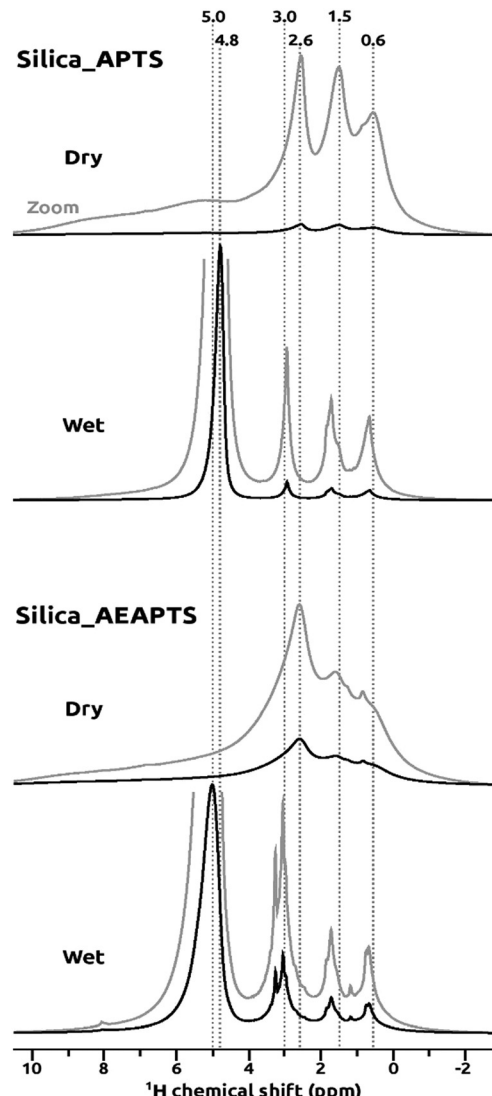


Fig. 2 ^1H NMR spectra in wet and dry conditions for samples modified with 3-aminopropyltriethoxysilane (Silica_APTS) and 3-(2-aminoethylamino)propyltriethoxysilane (Silica_AEAPTS) after being subjected to CO_2 . The grey lines correspond to a zooming of the black ones and fast magic-angle spinning of 60.0 kHz was used.

adsorption increase in this regime. For both amine modified silica samples, the CO_2 isotherms had a much larger gradient at low pressures than for the unmodified silica as shown in Fig. 3. The difference in gradients support established findings^{49,50} of a higher heat of chemisorption of CO_2 on amine modified silica than for physisorption of CO_2 on unmodified silica surfaces. On pure silica, CO_2 adsorbs by physisorption, which is mainly governed by electrostatic interaction between CO_2 and the silica surface.

The interaction is caused by the significant quadrupole moment of CO_2 molecules and the electrical field variation of the silica surface.⁵¹ On amine-modified silica, CO_2 chemisorbs, as discussed in sections above, and in the literature,^{14,15,25,27,46} as carbamate-ion pairs, carbamic acid or alike, or HCO_3^- depending on the properties of the sorbent and conditions

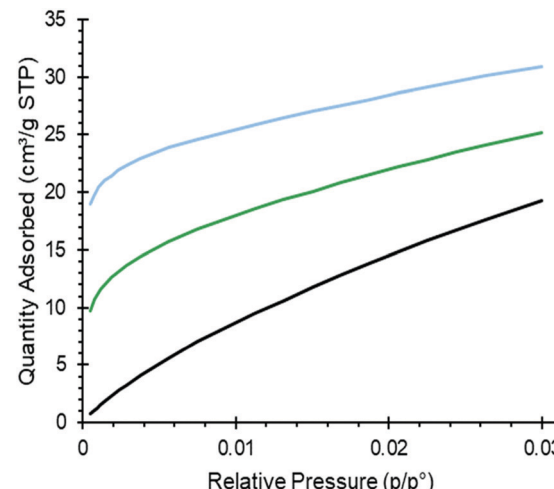


Fig. 3 CO_2 adsorption measurements at 0 °C. Black: pure silica; green: Silica_APTS; blue: Silica_AEAPTS.

applied. A very high uptake of CO_2 at a low pressure of CO_2 for Silica_APTS shows a synergistic effect with carbamates forming across different propyl amine groups, which has been shown to occur above a critical amine density for monoamines.^{49,52,53} The very high CO_2 uptake at a low pressure of CO_2 for Silica_AEAPTS relates to intramolecular (and possibly intermolecular) carbamates being formed, which has been shown by *e.g.* Lashaki *et al.*^{54,55}

4.3. Thermogravimetric analysis

The amount of organic groups in the Silica_APTS and Silica_AEAPTS were established with TGA by analyzing the mass loss recorded as the temperature increased within an appropriate temperature range. The temperature decomposition profiles can be seen in Fig. 4. From this, an estimation for the degree of modification of the amine-modified samples was extracted and

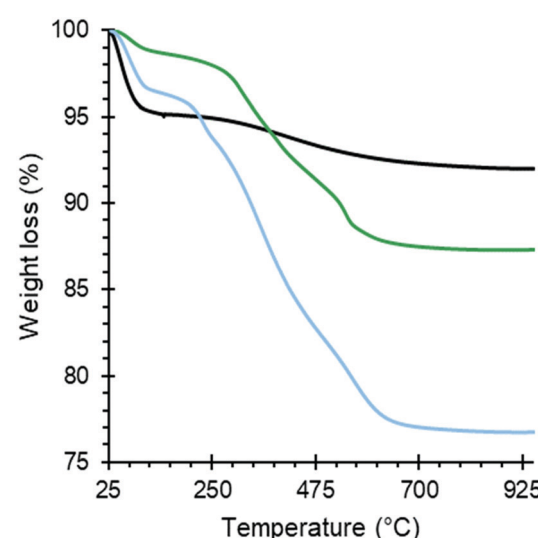


Fig. 4 TGA curves in dry air. Black: pure silica; green: Silica_APTS; blue: Silica_AEAPTS.



Table 1 Degree of modification deduced from TGA

Sample	Weight loss due to organics (%)	Monomer concentration (%)	Monomer/SiO ₂
Silica_APTS	11	13.1	7.5
Silica_AEAPTS	21	16	6.5

presented in Table 1. It is also important to note that the diaminated Silica_AEAPTS presented an increased capacity to chemisorption of CO₂ when compared to the monoaminated Silica_APTS, despite having a similar degree of modification molewise (Table 1), and simply ascribed to that each modification in the Silica_AEAPTS contained two reactive amine groups.

5. Conclusions

Here, mesoporous silica was modified with two different aminosilanes (the monoamine APTS and the diamine AEAPTS) and studied as CO₂ sorbents. Systematic solid state NMR experiments were performed to study how CO₂ chemisorbed under dry and moist conditions and the viability of using this technique under ultrahigh MAS conditions was tested. High quality spectra for both ¹³C and ¹H NMR were detected especially in the case of the moist samples.

For both modified samples, CO₂ chemisorbed as carbamic acid and carbamate ammonium ion pairs under dry conditions, and the directly-excited ¹³C and {¹H}¹³C MAS NMR spectra obtained were significantly similar. When the samples were allowed to equilibrate in a humid environment (wet samples), carbamate ammonium ion pairs were again detected together with significant amounts of HCO₃⁻ instead of carbamic acids, by using either direct excitation ¹³C or {¹H}¹³C NMR spectroscopy. The cross-polarization efficiency to the HCO₃⁻ was reduced as compared to the directly detected ¹³C NMR. Still, with pre-knowledge of this tendency of reduction, {¹H}¹³C NMR could be used to qualitatively establish the presence of HCO₃⁻ for these samples without having to cool them down. We predict that {¹H}¹³C NMR can be used for qualitative assessment of HCO₃⁻ also without isotopic ¹³C enrichment for similar samples, which would be convenient.

The presence of H₂O in the aminated samples lead to a sharpening of all signals (¹H and ¹³C) under rapid MAS, and the sharpening was ascribed to an enhanced mobility of the species. This sharpening allowed for detection of two different types of carbamates formed on chemisorption of CO₂ on the diaminated sample as well as resolving most of the signals from the alkyl chains in the ¹H domain. These high resolutions of the ¹H and ¹³C NMR spectra observed could open up for more understanding in the process of how amine-modified silicas capture CO₂, can allow a better and more rational application of them, and sharpen their use in other important fields such as in catalysis.

Conflicts of interest

There are no conflicts to declare.

Acknowledgements

This project was supported by the EU-MSCA-ETN-GreenCarbon project 721991. The Swedish Research Council and the grant 2016-03568 is thanked for partial support of this study.

References

- D. Aaron and C. Tsouris, *Sep. Sci. Technol.*, 2005, **40**, 321–348.
- H. Yang, Z. Xu, M. Fan, R. Gupta, R. B. Slimane, A. E. Bland and I. Wright, *J. Environ. Sci.*, 2008, **20**, 14–27.
- S. A. Didas, S. Choi, W. Chaikittisilp and C. W. Jones, *Acc. Chem. Res.*, 2015, **48**, 2680–2687.
- E. Andreoli, E. P. Dillon, L. Cullum, L. B. Alemany and A. R. Barron, *Sci. Rep.*, 2014, **4**, 1–5.
- J. F. Van Humberg, T. M. McDonald, X. Jing, B. M. Wiers, G. Zhu and J. R. Long, *J. Am. Chem. Soc.*, 2014, **136**, 2432–2440.
- X. Shi, H. Xiao, H. Azarabadi, J. Song, X. Wu, X. Chen and K. S. Lackner, *Angew. Chem., Int. Ed.*, 2020, **59**, 6984–7006.
- G. Zhao, B. Aziz and N. Hedin, *Appl. Energy*, 2010, **87**, 2907–2913.
- A. Goeppert, S. Meth, G. K. S. Prakash and G. A. Olah, *Energy Environ. Sci.*, 2010, **3**, 1949–1960.
- R. W. Flaig, T. M. O. Popp, A. M. Fracaroli, E. A. Kapustin, M. J. Kalmutzki, R. M. Altamimi, F. Fathieh, J. A. Reimer and O. M. Yaghi, *J. Am. Chem. Soc.*, 2017, **139**, 39.
- F. Y. Chang, K. J. Chao, H. H. Cheng and C. S. Tan, *Sep. Purif. Technol.*, 2009, **70**, 87–95.
- N. Hedin and Z. Bacsik, *Curr. Opin. Green Sustainable Chem.*, 2019, **16**, 13–19.
- S. Zhang, C. Chen and W. S. Ahn, *Curr. Opin. Green Sustainable Chem.*, 2019, **16**, 26–32.
- Y. Zhai, H. Jin and S. S. C. Chuang, *Chemistry of Silica and Zeolite-Based Materials*, Elsevier, 2019, pp. 121–142.
- J. K. Moore, M. A. Sakwa-Novak, W. Chaikittisilp, A. K. Mehta, M. S. Conradi, C. W. Jones and S. E. Hayes, *Environ. Sci. Technol.*, 2015, **49**, 13684–13691.
- Z. Bacsik, N. Ahlsten, A. Ziadi, G. Zhao, A. E. Garcia-Bennett, B. Martín-Matute and N. Hedin, *Langmuir*, 2011, **27**, 11118–11128.
- S.-J. Huang, C.-T. Hung, A. Zheng, J.-S. Lin, C.-F. Yang, Y.-C. Chang, F. Deng and S.-B. Liu, *J. Phys. Chem. Lett.*, 2014, **5**, 3.
- G. S. Foo, J. J. Lee, C.-H. Chen, S. E. Hayes, C. Sievers and C. W. Jones, *ChemSusChem*, 2017, **10**, 266–276.
- A. Danon, P. C. Stair and E. Weitz, *J. Phys. Chem. C*, 2011, **115**, 11540–11549.
- C. Knöfel, C. Martin, V. Hornebecq and P. L. Llewellyn, *J. Phys. Chem. C*, 2009, **113**, 21726–21734.
- N. Hiyoshi, K. Yogo and T. Yashima, *Microporous Mesoporous Mater.*, 2005, **84**, 357–365.
- D. J. Fauth, M. L. Gray, H. W. Pennline, H. M. Krutka, S. Sjöström and A. M. Ault, *Energy Fuels*, 2012, **26**, 2483–2496.

22 Y. Belmabkhout, R. Serna-Guerrero and A. Sayari, *Chem. Eng. Sci.*, 2010, **65**, 3695–3698.

23 S. A. Didas, M. A. Sakwa-Novak, G. S. Foo, C. Sievers and C. W. Jones, *J. Phys. Chem. Lett.*, 2014, **5**, 4194–4200.

24 V. Zelenak, D. Halamova, L. Gaberova, E. Bloch and P. Llewellyn, *Microporous Mesoporous Mater.*, 2008, **116**, 358–364.

25 A. C. C. Chang, S. S. C. Chuang, M. Gray and Y. Soong, *Energy Fuels*, 2003, **17**, 468–473.

26 C.-H. Yu, C.-H. Huang and C.-S. Tan, *Aerosol Air Qual. Res.*, 2012, **12**, 745–769.

27 C. H. Chen, D. Shimon, J. J. Lee, F. Mentink-Vigier, I. Hung, C. Sievers, C. W. Jones and S. E. Hayes, *J. Am. Chem. Soc.*, 2018, **140**, 8648–8651.

28 M. W. Hahn, M. Steib, A. Jentys and J. A. Lercher, *J. Phys. Chem. C*, 2015, **119**, 4126–4135.

29 X. Wang, V. Schwartz, J. C. Clark, X. Ma, S. H. Overbury, X. Xu and C. Song, *J. Phys. Chem. C*, 2009, **113**, 7260–7268.

30 G. Richner and G. Puxty, *Ind. Eng. Chem. Res.*, 2012, **51**, 14317–14324.

31 R. Zhang, Z. Liang, H. Liu, W. Rongwong, X. Luo, R. Idem and Q. Yang, *Ind. Eng. Chem. Res.*, 2016, **55**, 3710–3717.

32 X. Yang, R. J. Rees, W. Conway, G. Puxty, Q. Yang and D. A. Winkler, *Chem. Rev.*, 2017, **117**, 9524–9593.

33 D. Bernin and N. Hedin, *Curr. Opin. Colloid Interface Sci.*, 2018, **33**, 53–62.

34 C.-H. Chen, D. Shimon, J. J. Lee, S. A. Didas, A. K. Mehta, C. Sievers, C. W. Jones and S. E. Hayes, *Environ. Sci. Technol.*, 2017, **51**, 26.

35 P. Rzepka, Z. Bacsik, A. J. Pell, N. Hedin and A. Jaworski, *J. Phys. Chem. C*, 2019, **123**, 21497–21503.

36 F. Mani, M. Peruzzini and P. Stoppioni, *Green Chem.*, 2006, **8**, 995–1000.

37 R. W. Flaig, T. M. Osborn Popp, A. M. Fracaroli, E. A. Kapustin, M. J. Kalmutzki, R. M. Altamimi, F. Fathieh, J. A. Reimer and O. M. Yaghi, *J. Am. Chem. Soc.*, 2017, **139**, 12125–12128.

38 B. Aziz, G. Zhao and N. Hedin, *Langmuir*, 2011, **27**, 3822–3834.

39 T. L. Hwang, P. C. M. Van Zijl and M. Garwood, *J. Magn. Reson.*, 1998, **133**, 200–203.

40 G. Kervern, G. Pintacuda and L. Emsley, *Chem. Phys. Lett.*, 2007, **435**, 157–162.

41 B. M. Fung, A. K. Khitrin and K. Ermolaev, *J. Magn. Reson.*, 2000, **142**, 97–101.

42 T. Čendak, L. Sequeira, M. Sardo, A. Valente, M. L. Pinto and L. Mafra, *Chem. – Eur. J.*, 2018, **24**, 10136–10145.

43 C. Te Hung, C. F. Yang, J. S. Lin, S. J. Huang, Y. C. Chang and S. Bin Liu, *Microporous Mesoporous Mater.*, 2017, **238**, 2–13.

44 M. L. Pinto, L. Mafra, J. M. Guil, J. Pires and J. Rocha, *Chem. Mater.*, 2011, **23**, 1387–1395.

45 L. Mafra, T. Čendak, S. Schneider, P. V. Wiper, J. Pires, J. R. B. Gomes and M. L. Pinto, *J. Am. Chem. Soc.*, 2017, **139**, 389–408.

46 P. V. Kortunov, M. Siskin, L. S. Baugh and D. C. Calabro, *Energy Fuels*, 2015, **29**, 5919–5939.

47 L. Phillips, F. Separovic, B. A. Cornell, J. A. Barden and C. G. dos Remedios, *Eur. Biophys. J.*, 1991, **19**, 147–155.

48 F. Rezaei, R. P. Lively, Y. Labreche, G. Chen, Y. Fan, W. J. Koros and C. W. Jones, *ACS Appl. Mater. Interfaces*, 2013, **5**, 3921–3931.

49 Z. Bacsik, R. Atluri, A. E. Garcia-Bennett and N. Hedin, *Langmuir*, 2010, **26**, 10013–10024.

50 M. W. Hahn, J. Jelic, E. Berger, K. Reuter, A. Jentys and J. A. Lercher, *J. Phys. Chem. B*, 2016, **120**, 1988–1995.

51 R. Roque-Malherbe, R. Polanco-Estrella and F. Marquez-Linares, *J. Phys. Chem. C*, 2010, **114**, 17773–17787.

52 P. D. Young and J. M. Notestein, *ChemSusChem*, 2011, **4**, 1671–1678.

53 B. Aziz, N. Hedin and Z. Bacsik, *Microporous Mesoporous Mater.*, 2012, **159**, 42–49.

54 M. Jahandar Lashaki, S. Khiavi and A. Sayari, *Chem. Soc. Rev.*, 2019, **48**, 3320–3405.

55 M. A. Alkhabbaz, P. Bollini, G. S. Foo, C. Sievers and C. W. Jones, *J. Am. Chem. Soc.*, 2014, **136**, 13170–13173.